PROTEINS
STRUCTURE ■ FUNCTION ■ BIOINFORMATICS

Quaternary structure effects on the hexacoordination equilibrium in rice hemoglobin rHb1: Insights from molecular dynamics simulations

Uriel N. Morzan,[1] Luciana Capece,[1] Marcelo A. Marti,[1,2]* and Dario A. Estrin[1]*

[1] Departamento de Química Inorgánica, Analítica y Química Física/ INQUIMAE-CONICET, Facultad de Ciencias Exactas y Naturales, Universidad de Buenos Aires, C1428EHA, Buenos Aires, Argentina

[2] Departamento de Química Biológica, Facultad de Ciencias Exactas y Naturales, Universidad de Buenos Aires, Ciudad Universitaria, Pabellón 2, Buenos Aires C1428EHA, Argentina

ABSTRACT

Nonsymbiotic hemoglobins (nsHbs) form a widely distributed class of plant proteins, which function remains unknown. Despite the fact that class 1 plant nonsymbiotic hemoglobins are hexacoordinate (6c) heme proteins (hxHbs), their hexacoordination equilibrium constants are much lower than in hxHbs from animals or bacteria. In addition, they are characterized by having very high oxygen affinities and low oxygen dissociation rate constants. Rice hemoglobin 1 (rHb1) is a class 1 nonsymbiotic hemoglobin. It crystallizes as a fully associated homodimer with both subunits in 6c state, but showing slightly different conformations, thus leading to an asymmetric crystallographic homodimer. The residues that constitute the dimeric interface are conserved among all nsHbs, suggesting that the quaternary structure could be relevant to explain the chemical behavior and biological function of this family of proteins. In this work, we analyze the molecular basis that determine the hexacoordination equilibrium in rHb1. Our results indicate that dynamical features of the quaternary structure significantly affect the hexacoordination process. Specifically, we observe that the pentacoordinate state is stabilized in the dimer with respect to the isolated monomers. Moreover, the dimer behaves asymmetrically, in a negative cooperative scheme. The results presented in this work are fully consistent with our previous hypothesis about the key role played by the nature of the CD region in determining the coordination state of globins.

Proteins 2013; 81:863–873.

Key words: nonsymbiotic hemoglobins; plant hemoglobins; rice hemoglobin 1; hexacoordination; molecular dynamics; heme protein; neuroglobin; cytoglobin; steered molecular dynamics.

INTRODUCTION

Hemoglobins are a large group of proteins responsible of a great variety of biological functions in all kingdoms of life.[1–3] Many of these functions are related with the capability to coordinate small ligands to the heme group.[4] The iron in the heme group possesses six coordination sites: four equatorial sites occupied by the porphyrin pyrrole nitrogens and two axial sites. One of the axial sites, known as proximal site is usually occupied in hemoglobins by a histidine residue. The sixth coordination site is known as the distal position. In many cases, this site is occupied by exogenous ligands such as O_2, CO, and NO. Several hemoglobins also contain a histidine (HisE7) called distal residue, which contributes to stabilize the heme–ligand complex through hydrogen bonding.[5] In some cases, however, this residue is also capable of binding to the iron leading to the formation of a hexacoordinated (6c) globin (hxHb), as observed in human neuroglobin,[6] human cytoglobin,[7] rice hemoglobin,[8] and tomato hemoglobin[9] among others.

To bind exogenous ligands, the so-called 6c globins need to populate at least transiently the pentacoordinate state (5c). This leads to the existence of a subtly regulated equilibrium between these states, that results in

Additional Supporting Information may be found in the online version of this article.

Luciana Capece's current address is German Research School for Simulation Sciences, D-52425 Jülich, Germany, International Centre for Genetic Engineering and Biotechnology, 34012 Trieste, Italy

*Correspondence to: Dario A. Estrin, Departamento de Química Inorgánica, Analítica y Química Física/INQUIMAE-CONICET, Intendente Güiraldes 2160, Ciudad Universitaria, C1428EGA, Argentina. E-mail: dario@qi.fcen.uba.ar or Marcelo A. Marti. E-mail: marcelo@qi.fcen.uba.ar
Received 13 July 2012; Revised 11 December 2012; Accepted 14 December 2012
Published online 27 December 2012 in Wiley Online Library (wileyonlinelibrary.com).
DOI: 10.1002/prot.24245

hexacoordinated hemoglobins displaying moderate O_2 affinities, as noted for neuroglobin ($P_{50} \approx 2$ torr).[10]

In the vegetal kingdom, there are three known types of hemoglobins: symbiotic hemoglobins (sHb), truncated hemoglobins (trHb), and nonsymbiotic hemoglobins (nsHb). The last two types have been recently discovered.[11] While symbiotic hemoglobins are 5c and found in nodules of nitrogen-fixing plants, nonsymbiotic hemoglobins are 6c and are present in all plants. Although it has been proven that their expression is enhanced under hypoxic conditions,[12] their physiological function is still unclear. Three classes (class 1, 2, and 3) of nsHbs have been distinguished.[13] Class 1 hemoglobins are found in all plants and are characterized by having much lower hexacoordination equilibrium constants than in hxHbs from animals or bacteria ($K_h \approx 2$) high oxygen affinities ($P_{50} \approx 2$ n*M*), and low oxygen dissociation rate constant ($K_D \approx 0.16\ s^{-1}$).[14–18] This behavior can be explained by the fact that the distal histidine stabilizes the bound ligand.[16] Several observations as low concentrations *in vivo*, small oxygen dissociation rate constants, high oxygen affinity and redox potential suggest that class 1 nsHbs are unlikely to function in oxygen or electron transport.[16,19,20]

Rice contains four nsHbs,[21] two of which have been studied in purified recombinant form (riceHb1 and riceHb2). It was postulated that they could be involved in energy maintenance and NADH reduction. This hypothesis is consistent with the upregulation observed in plants grown under stress conditions.[22,23] In addition, for rice rHb1 genes are induced by nitrate, nitrite, and nitric oxide donors in association with NADH-nitrate reductase.[24] This suggests that rHb1 could be involved in nitric oxide scavenging detoxification.[25]

The crystal structure of rHb1 has been solved by Hargrove *et al.*[8] It crystallizes as a fully associated dimer with both subunits in 6c state (bis-histidil-6c state).[8] Under physiological conditions, it is a partially associated homodimer (K_d = 80–610 μM depending on the oxidation states and the ligand bound of the heme group).[26] The tertiary structure consists of six helices commonly named A, B, E, F, G, and H present in most hemoglobins (Fig. 1). The crystal structure shows a very short and distorted C helix. The D helix region forms an extended and poorly ordered loop suggesting that the CD region may be highly flexible under physiological conditions. It was also observed that residue Phe40(B10), which is conserved in plant nonsymbiotic hemoglobins, displays a great variability in its side chain position. Interestingly, studies by Smagghe *et al.* have identified this residue as an important regulatory element in hexacoordination and ligand binding.[27]

The dimeric interface observed in the crystal structure is symmetrical, and it is formed by amino acids from the CD region and the G helix. More specifically, the interactions observed between the two subunits are two hydrogen bonds between Ser49 from one subunit and the Glu119 from the other and a hydrophobic core formed by Phe123, Val120, and Val46. Residues Ser49, Glu119, Val46, and Val120 have shown to play a critical role in the formation of the quaternary structure. These residues are relatively conserved among all the nsHbs[8] suggesting that this quaternary structure could be relevant to explain the chemical behavior and biological function of this family of proteins. Interestingly, both subunits (labeled A and B) display different structures. The backbone root mean square deviation (RMSD) between the two monomers is 1.6 Å. Specific backbone structural differences between the two monomers are found mainly in the loop CD conformation but also in the F helix.[8] This kind of asymmetry has also been reported to be present in several, in principle symmetric, protein homodimers.[28–30]

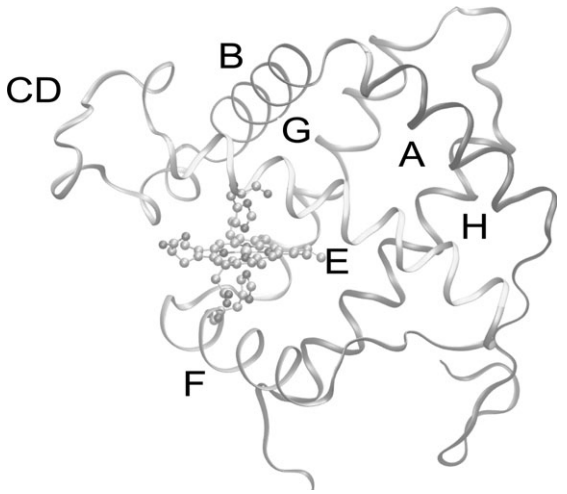

Figure 1

Visual representation of the monomeric rHb1 structure. The heme is depicted in balls and sticks drawing representation and the rest of the protein is in ribbon representation.

In previous works, our group has pointed out the crucial role of the CD region as the main determinant of the equilibrium in human neuroglobin.[31,32] In the present work, we analyze the molecular basis that determine the hexacoordination equilibrium in rHb1 and its connection with the quaternary structure. Our results indicate that quaternary structure affects significantly the hexacoordination process. Specifically, we observed that the 5c state is stabilized by dimerization, which means that the role played by the dimeric interface could be related to the modulation of the hexacoordination equilibrium. Our results are fully consistent with our previous hypothesis about the key role played by the nature of the CD region in determining the coordination state of globins.[31,32]

MATERIALS AND METHODS

Starting structures

The initial structure of rHb1 was obtained from X-ray structures (PDB entries 1D8U[8]). The 5c structures were

obtained from the 6c one by releasing the Fe-HisE7 bond constraint followed by 5-ns MD simulations, which promotes distal histidine dissociation from the heme. For each one of the monomeric subunits of rHb1, 50-ns MD simulation was performed in all the possible coordination states. Four MD trajectories were run corresponding to 5c-A, 6c-A, 5c-B, and 6c-B (where the labels A and B correspond to each chain in the dimer). For the dimeric state, 60-ns MD simulation trajectories were collected for the A6c–B6c and A5c–B5c. In the case of A6c–B5c and A5c–B6c states, 65-ns and 70-ns MD simulations were collected, respectively.

Simulation parameters

The starting structures were immersed in a pre-equilibrated octahedral box of TIP3P water molecules. A minimum distance of 15 Å from the protein surface to the end of the box was used. This resulted in a total number of 27,794 atoms for the monomers and 40,939 atoms for the dimers. The standard protonation state at physiological pH was assigned to ionizable residues. Histidine residues protonation were assigned on the basis of the hydrogen-bond pattern with neighboring residues. For distal (HisE7) and proximal (HisF8) histidines, protonation was chosen to be in the Nδ position. All simulations were performed at 300 K and pressure of 1 bar using Berendsen thermostat and barostat.[33] Periodic boundary conditions and Ewald sums (grid spacing of 1 Å) were used to treat long-range electrostatic interactions. The SHAKE algorithm was used to keep bonds involving hydrogen atoms at their equilibrium length. The time step for the integration of Newton's equations was 2 fs. The force field used for all residues but the heme was Amber99.[34] Heme parameters were developed and thoroughly tested by our group in previous works.[31,32,35,36] All simulations were performed with the PMEMD module of the AMBER10 package.[37] Frames were collected at 1-ps intervals, which were subsequently used to analyze the trajectories. The equilibration protocol consisted in an energy minimization of the initial X-ray structures, followed by a gradual heating up to 300 K (four steps of 5 ps at 150, 200, 250, and 300 K). For each structure, the first 15 ns were not considered for further analysis.

Essential dynamics

Essential dynamics (ED) analysis involves diagonalization of the covariance matrices of atomic positions along the trajectory, yielding the eigenvectors that define the essential motions of the protein.[38] This analysis was performed only for the backbone atoms. Residues 1–15 and 150–165 were excluded to avoid masking of the essential motions of the protein core by the high flexibility of the terminal regions. ED analysis of combined trajectories (6c and 5c) was also performed to gain insight into the structural transition.[31] This type of analysis has been successfully applied in previous works to study conformational transitions, including 5c ↔ 6c equilibrium in globins, allowing the understanding on how protein structure and dynamics contributes to the conformational change process.[31,32,39]

Free energy profiles of the 5c↔6c transition

To obtain thermodynamic information of the 5c ↔ 6c transition, free energy profiles for this process were calculated. The profiles were constructed by performing constant velocity multiple steered molecular dynamics simulations by means of the PMEMD module of Amber10 program, and using the Jarzinsky's equation.[40] Here, the reaction coordinate was chosen as the Fe-Nϵ2(HisE7) distance. Calculations were performed using a harmonic potential with a force constant of 400 kcal mol^{-1} $Å^{-1}$ on the Fe-Nϵ2 distance and pulling velocities of 2.5 Å ns^{-1}. Twenty simulations were performed in each direction. The final profile in each case was obtained by combining the forward and backward profiles (forward = dissociation and backward = association). As the coordination transition involves the formation/breaking of a bond (the Fe-HisE7 bond), a process not allowed in standard classical force fields, we introduced a Morse potential to describe such Fe-coordination bond. The parameters in this case are an equilibrium distance of 2.01 Å and a bond dissociation energy of 10 kcal mol^{-1}. This set of parameters have been used in previous works to study this process in other globins.[31,32] It is important to stress out that the Morse potential function that describes the Fe-HisE7 bond was not parameterized for this case in particular but for a generic hxHb case. Therefore, we do not expect quantitative accuracy for any individual profile but just a meaningful comparison between different states. This scheme has been successfully applied to the determination of free energy profiles in proteins for a wide variety of processes including 5c ↔ 6c transition in globins.[31,32,41–44]

RESULTS

Structural and dynamical analysis of rHb1 in the dimeric state

To study the structural properties of dimeric rHb1, four MD simulations, were performed corresponding to each one of the possible coordination states, namely: A5c–B5c, A6c–B6c, A6c–B5c, and A5c–B6c (where 5c and 6c indicate the coordination states and letters A and B are the labels that distinguish each subunit in the asymmetric dimer). In all cases, no large structural fluctuations were observed during the time scale of the simulation, as evidenced in the RMSD versus time (Supporting Information Figs. S1 and S2). The RMSD between the average structures of subunits A and B in

the A6c–B6c state (which is the coordination state of the crystal structure) resulted 3.8 Å (compared with 1.6 Å in the crystal structure).

A more detailed analysis of the protein mobility is obtained by the root mean square fluctuation (RMSF) versus residue plot, which shows that the more mobile protein regions are located in the loops AB, EF, GH, and particularly in the CD region (Fig. 2). Noteworthy, the figure also shows that the mobility of the CD region is higher in subunit B compared to subunit A, specially in the cases where subunit A is in the 6c state.

The ED analysis for the hexacoordination process in the dimeric state shows that the structural rearrangements that take place during the hexacoordination in each subunit are mainly associated with a conformational reorganization of the CD region and the F helix (Supporting Information Fig. S9).

Another relevant observation derived from Figure 2, is that in the A6c–B6c state [Fig. 2(B)], the GH loop of subunit A shows a significantly higher mobility compared to any of the other simulated states. Visual inspection of the MD trajectory evidences that this effect is related with the dimeric interface and is caused by the vicinity of B subunit's CD region to the H helix of subunit A, which allows the formation of two hydrogen bonds, established between Ser60 and Arg58 from subunit B with Ser144 and Glu148 from subunit A, respectively, as shown in Figure 3(A,B). This contact also allows the hydrogen bonding between Ser55 and Glu65 residues from subunit B's CD region. The existence of this interaction between the GH loop of subunit A and the CD region of subunit B may explain the observed increase in the GH flexibility, due to the high flexibility of the CD region. These interactions [shown in Fig. 3(B)] are mostly found in both the A6c–B6c and A5c–B6c dimer, and thus are particular of B6c state. In contrast, in the dimeric states in which subunit B is in the 5c state, its CD region does not interact with subunit A at all. Instead, a hydrophobic core between the apolar amino acids in this region is formed, as shown in Figure 3(C,D). In summary, there is a B subunit coordination dependent, differential interaction with subunit A. On the other hand, subunit A CD region forms a compact hydrophobic core, whose behavior seems to be independent with the other subunit.

Another interesting observation is that in both subunits and both states, the side chain of PheB10 can have two very distinct orientations as shown in Figure 4(B). The first one is in the distal pocket direction near the distal histidine (closed orientation), and in the second, it points toward the opposite way (open orientation). In Figure 4(B), it can be observed that in the closed orientation the distal histidine is severely hindered by PheB10, while in the open orientation, the distance between both residues is always higher than 5 Å. This effect is a potential modulator of the 5c–6c transition, given that in the

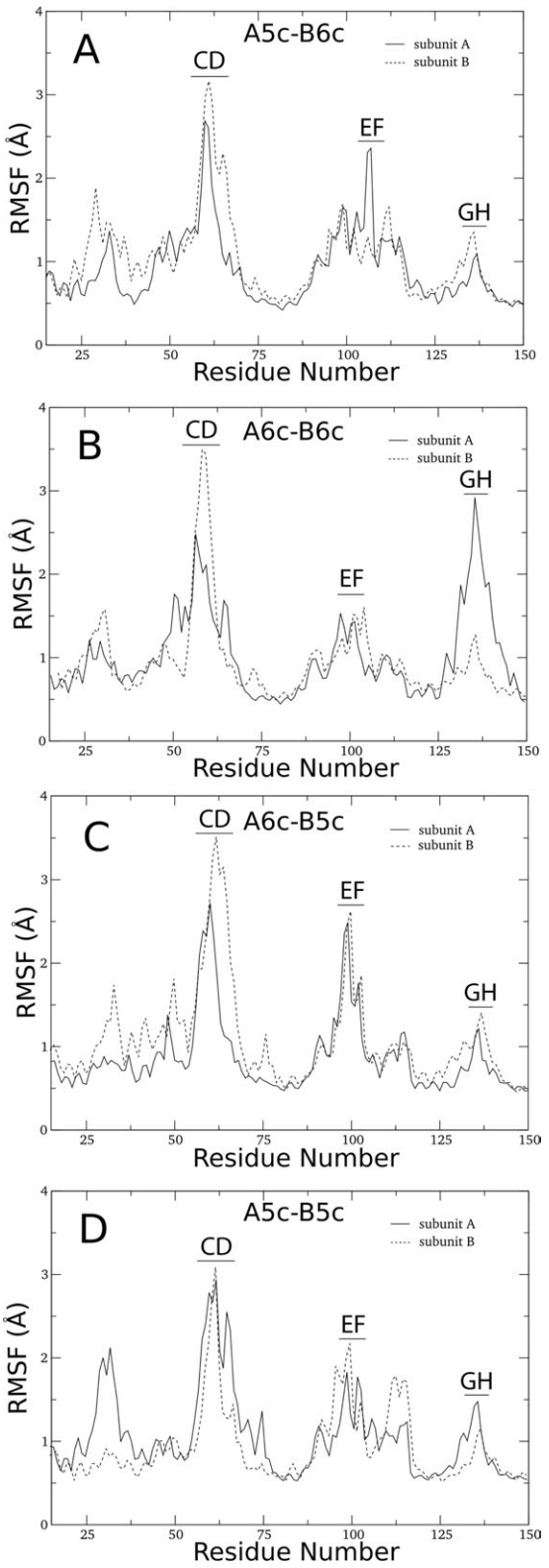

Figure 2

RMSF as a function of the residue number for each of the rHb1 monomers, computed for each possible dimer state simulation. The results shown in each panel correspond to the following configurations: (**A**) A5c–B6c; (**B**) A6c–B6c; (**C**) A6c–B5c; (**D**) A5c–B5c.

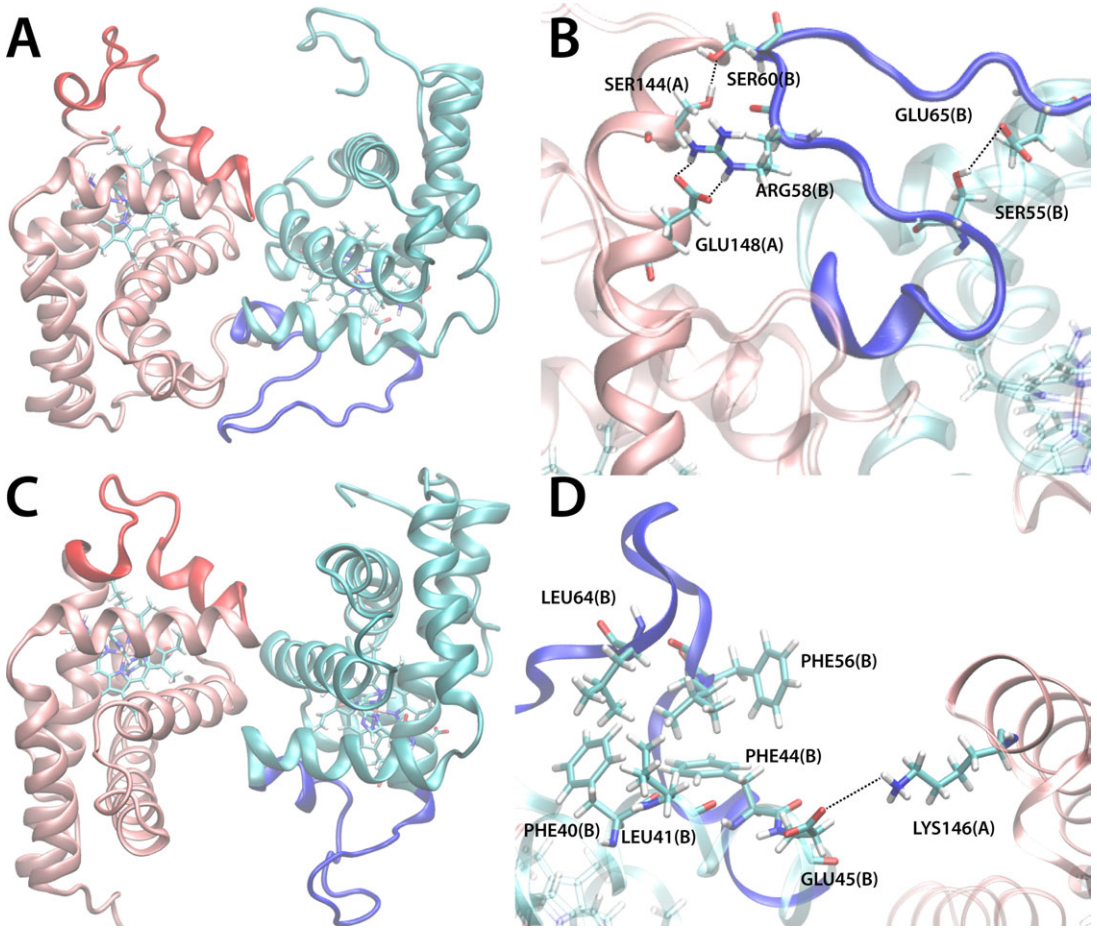

Figure 3

MD trajectory analysis of the dimer. Subunit A is represented in pink color and subunit B is in cyan. CD regions are represented in red and blue for subunit A and B, respectively. (**A**) Representative snapshot from A6c–B6c dimer. (**B**) Interactions between subunit B's CD region (blue) with residues from subunit A's H helix (Pink) in A6c–B6c dimer. These interactions consist in three hydrogen bonds between Ser60 and Arg58 from subunit B's CD region with Ser144 and Glu148 from subunit A's H helix. This movement of the CD region also allows the formation of a hydrogen bond between Glu65 with Ser55 in subunit B. (**C**) Selected snapshot from A6c–B5c dimer. (**D**) Hydrophobic interactions between residues in subunit B's CD region in A6c–B5c dimer.

5c state, the distal histidine is slightly displaced away from the heme. Thus, PheB10 could play the role of modulating the 5c state stability.

To explore the possible interplay between PheB10 conformation and hexacoordination equilibrium, we analyzed the populations of the PheB10 opened and closed states. Interestingly, as illustrated in Table I, both subunits display a clear differential preference for the closed orientation of PheB10 when the other subunit is in the 5c state. On the other hand, the population of PheB10 in the opened orientation in each subunit is highly increased when the other subunit is in the 6c state, with the notable exception of the A5c–B5c state, where PheB10 residue presents a clear predominance of the opened orientation in subunit B and closed orientation in subunit A.

A feasible mechanism whereby a change in the coordination state of each subunit results in a modification of PheB10 side chain orientation in the other subunit, could be related with the structural differences that exist between each subunit 5c and 6c states. Figure 4(B) shows a comparison between the behavior of the F helix and the heme in the 5c and 6c states of subunit A, in the A5c–B6c and A6c–B6c dimers. As can be observed, in the 5c state the distal histidine rotates towards the distal pocket allowing a small sliding of the heme. This movement of the heme also forces the F helix to change its position through the bound proximal histidine. The movement of the F helix, alters the relative position of the G helix. In particular, residues Phe123 and Val120 that compose the dimeric interface, and that are directly bound with Val46 (B16) generating a displacement in the B helix of the other subunit, where PheB10 is located [Fig. 4(C)]. The magnitude of the displacements caused by hexacoordination in the residues involved in the

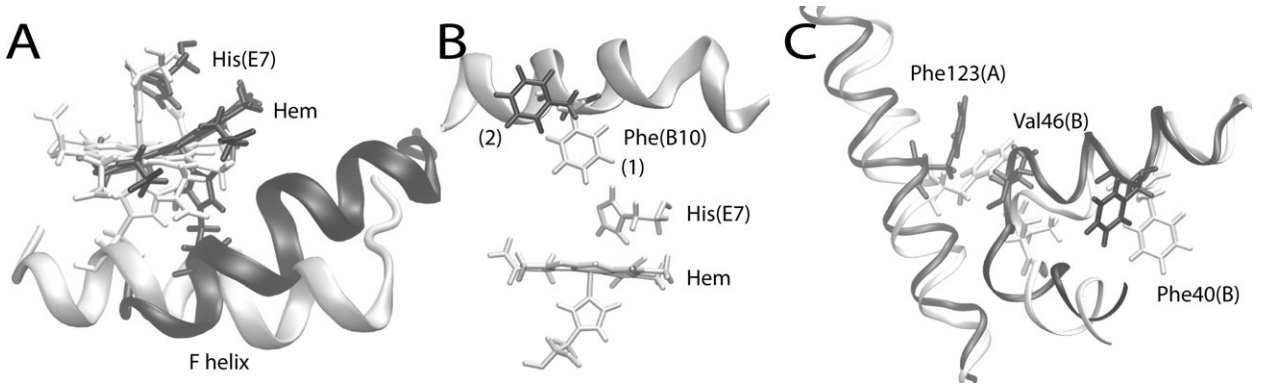

Figure 4

(**A**) Superposition of representative snapshots of subunit A in the simulation obtained for A6c–B6c (white) and A5c–B6c (black) dimers. The F helix is observed in ribbon representation, distal and proximal histidines and the heme are in licorice representation. (**B**) Representative snapshot of subunit B in the 5c state. The two possible orientations for the residue PheB10 are shown. The first position (white) and the second one (black) are obtained from A5c–B5c and A6c–B5c simulations, respectively. (**C**) Superposition of representative snapshots of subunit B fixing A in 5c state (white) and 6c state (black). The heme exhibits the connection between the structural orientation of PheB10 (1 = "closed orientation" and 2 = "open orientation") and the dimeric interface residues Phe123 and Val46.

dimeric interface are shown in Supporting Information Table S10.

The observations described and analyzed above suggest that in rHb1 the dimeric interface and the CD region, display a dynamical behavior, which is conditioned by the coordination state of each subunit heme group. Moreover, it may constitute a mechanism whereby the quaternary structure modulates the 5c–6c transition equilibrium. This modulation can be achieved not only because PheB10 can directly influence the dissociation of the distal histidine from the heme to reach the 5c state, but also due to the fact that, as observed in previous works,[14,31,32] changes in the CD region conformation (as those caused by the dimeric interface described above) can produce a shift in the 5c–6c transition free energy.

Free energy profiles for the 5c ↔ 6c transitions in the dimer

To get a thermodynamic and kinetic prospect on the hexacoordination equilibrium, the free energy profiles corresponding to the 5c ↔ 6c transition were calculated for all the possible coordination states of the dimer. The complete results are shown in Figure 5. The free energy profile observed for subunit A, suggests that the thermodynamic hexacoordination tendency is poorly influenced by the coordination state of subunit B (Fig. 5, upper panel). Thus, the reorientation of PheB10 described in the previous section does not seem to affect significantly the hexacoordination kinetics or equilibrium in subunit A. In contrast, the free energy profiles for subunit B revealed a behavior consistent with the hypothesis that the hexacoordination equilibrium is altered by the position of PheB10 (Fig. 5, lower panel). As observed in Figure 4(B), 5c state is stabilized when subunit A is in 6c state (open orientation of PheB10) or destabilized if subunit A is in 5c state (closed orientation of PheB10). In other words, subunit B presents a coordination behavior that seems to depend on the PheB10 side chain orientation, but more important it seems to depend on the coordination state of subunit A in a sort of negative cooperativity scheme (i.e., 5c state is stabilized in subunit B, when subunit A is 6c or destabilized when subunit A is 5c). Noteworthy, this observation supports the hypothesis that the asymmetrical properties of the dimeric interface modulate the hexacoordination equilibrium.

One interrogation that arises here is how can the hexacoordination equilibrium be highly dependent on the orientation of PheB10 in one subunit and apparently have no influence in the other? A possible explanation for this difference relies on the size and shape of the distal cavity, which is partially defined by the CD region structure, that defines the presence of different subunit conformations. In subunit A, the distal cavity is much more compact and rigid than in subunit B. When PheB10 is in the open orientation, PheB9 partially

Table I
Open and Closed PheB10 Conformation Populations for Each State of the Dimer

	A		B	
	Closed (%)	Opened (%)	Closed (%)	Opened (%)
A6c–B6c	2	98	0	100
A5c–B6c	5	95	88	12
A6c–B5c	99	1	0	100
A5c–B5c	90	10	17	83

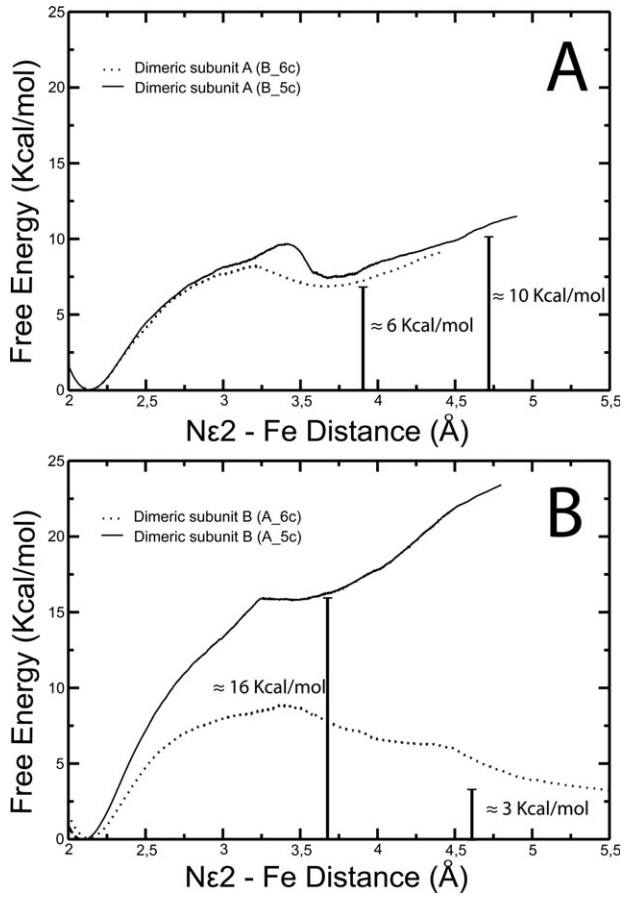

Figure 5

Free energy profile for the5c ↔ 6ctransition for subunit A (**A**) and B (**B**). A: Dashed line corresponds to A6c – B5c ↔ A5c – B5c process. Dotted line corresponds to A6c – B6c ↔ A5c – B6c process. B: Dotted line corresponds to A6c – B6c ↔ A6c – B5c process. Dashed line corresponds to A5c – B6c ↔ A5c – B5c process.

occupies the space region occupied by the side chain of PheB10 in the closed orientation. In fact, the equilibrium Fe–Nϵ2 distance in the 5c state is around 3.8 Å in subunit A and 5.5 Å in subunit B (A6c–B5c dimer) (Fig. 5). Thus, it is possible that the more compact conformation of the CD region and distal pocket produces a steric hindrance that prevents the distal histidine in subunit A to reach the same equilibrium position observed for subunit B.

Structural and dynamical analysis of the monomeric state

Despite the absence of an initial X-ray structure and the consequent lack of a starting monomeric state for the simulations, the initial conformation of the monomer was obtained from the dimeric initial structure by a standard relaxation and thermalization protocol (see computational methods). MD simulation (50 ns) of the monomeric conformations obtained from each subunit in rHb1 homodimer (conformations A and B) were performed in the two possible coordination states, 5c and 6c. Four MD trajectories were collected corresponding to 5c-A, 6c-A, 5c-B, and 6c-B (where 5c and 6c indicate the coordination state and the conformations where labeled as A and B in correspondence to each initial subunit conformation, as found in the dimer). In all cases, the structure of the protein remains stable and no large conformational changes are observed during the simulation, as noted in the positional root mean square deviation (RMSD) (See Supporting Information Fig. S2). The calculated RMSD along the MD trajectory also show larger fluctuations in the B conformation for both coordination states, indicating a higher flexibility than that observed for conformation A. Visual inspection of the MD trajectories and the calculated RMSF values per residue indicate that the most important structural differences between the conformations A and B are located in the CD region (Fig. 6). This is reasonable considering that the CD region is the most flexible part of the protein, followed by the EF and GH corners. Moreover, while in 5c-A and 6c-A short C and D helices can be observed in 5c-B and 6c-B case, the CD region is unusually extended and completely unwound. In both cases, the PheB10 residue is capable of exploring both the open and close orientations observed for the dimer.

It is reasonable to expect that simulations of the monomer, no matter the initial structure used, would yield the same results, provided that a sufficiently long simulation is performed. However, during the time scale of our simulations, interconversion between A and B subunit type conformations is not observed. Thus, all monomeric states remain in a similar conformation to the starting one. Nevertheless, based on the fact that the total surface area buried by dimeric interface is at the lower end of what is expected for a stable dimer,[8] it is reasonable to assume that these two conformations (A and B) could be taken as possible representative monomeric states.

Figure 6 highlights the differences between the two monomeric conformations and how the coordination state affects it. First, the CD region is more flexible in the conformation B than in the A case for both coordination states. Moreover, while 6c-A state shows a moderate increase in CD region's flexibility with respect to the 5c state, 5c-B and 6c-B states have similar suppleness in this region. This result implies that the differences observed between conformations A and B are crucial in determining the way through which hexacoordination modifies the protein structure.

Essential dynamics analysis for the monomeric conformations

The essential motions along the MD trajectory of each one of the monomeric conformations were obtained for

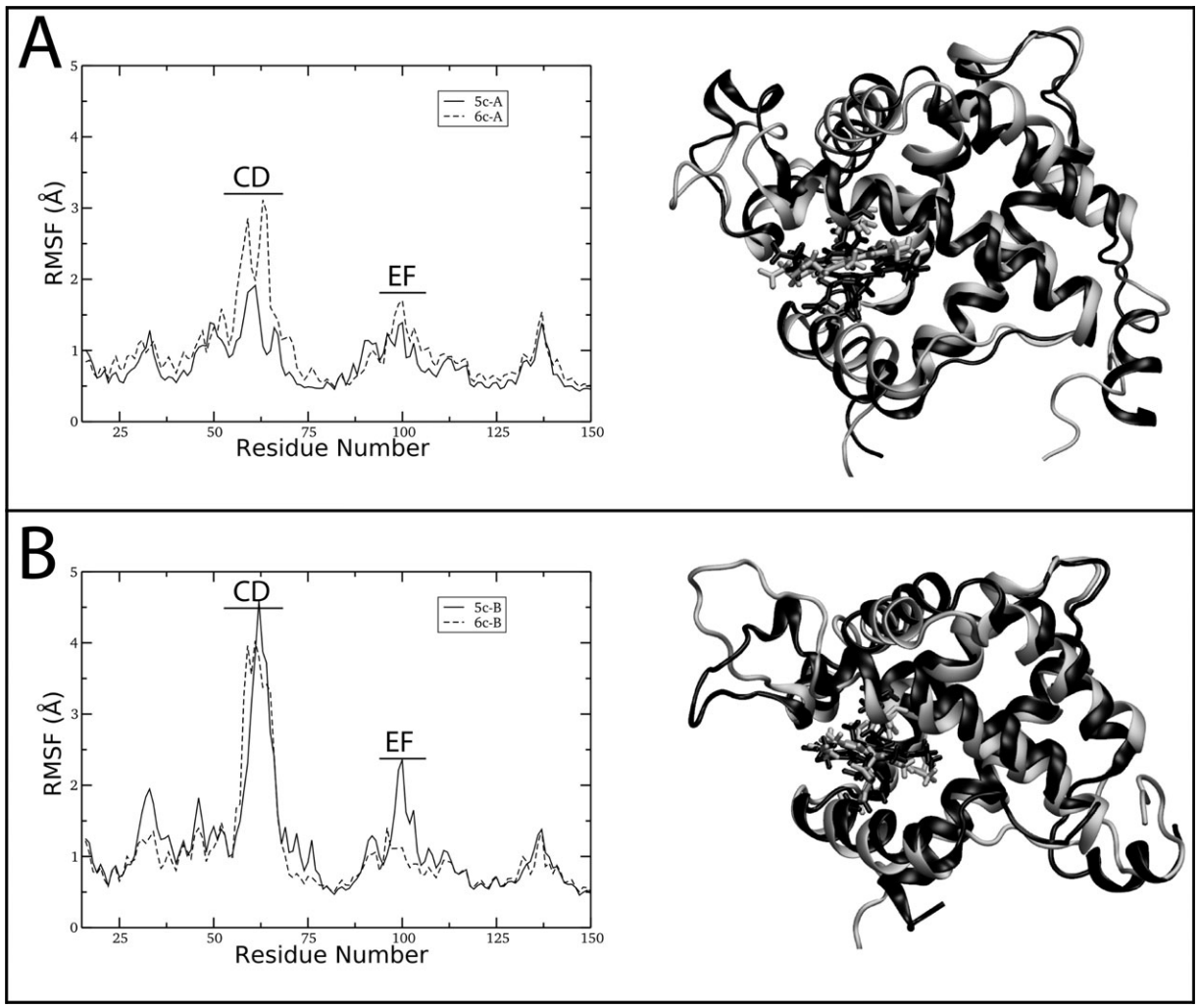

Figure 6

MD trajectory analysis of each one of the monomeric conformations. **A** (left): Root-mean-square-fluctuation along the protein sequence for conformation A; (right): representative snapshot obtained from conformation A MD trajectories. The 6c state is displayed in black and 5c state is displayed in gray. **B** (left): Root-mean-square-fluctuation along the protein sequence for conformation B; (right): representative snapshot obtained from conformation B MD trajectories. The 6c state is displayed in black and 5c state is displayed in gray.

both the 5c and 6c states to examine the structural changes associated with the hexacoordination process. In all cases, the contribution of the first three essential modes to the overall protein motion is higher than 55%. As expected, these results show that for the 6c state both subunits display first three essential modes mainly located in the CD region. In contrast, the 5c state shows for both A and B conformations, essential motions that include important contribution from the EF loop.

To further analyze the 5c ↔ 6c transition, the essential modes corresponding to this process were derived by combining the 5c and 6c trajectories.[32] Interestingly, the transition mode of both subunits mainly involves a conformational rearrangement mostly limited to the CD region and at less extent the EF fragment (Fig. 7).

Free energy profiles for the 5c ↔ 6c transitions in the monomer

As in the dimer's case, to characterize the hexacoordination equilibrium in the monomer, free energy profiles for this process were obtained for each monomeric conformation. Figure 8 shows that despite the structural differences observed between A and B conformations, the activation and the overall free energy difference for the 5c → 6c process are very similar for both conformations. The relevance of this result relies on the comparison between monomeric and dimeric free energy profiles. In the first case, the profiles of each one of the monomeric conformations indicate that the predominant state is by far the 6c. On the other hand, in the dimer 5c state seems to be stabilized in the mixed coordination state

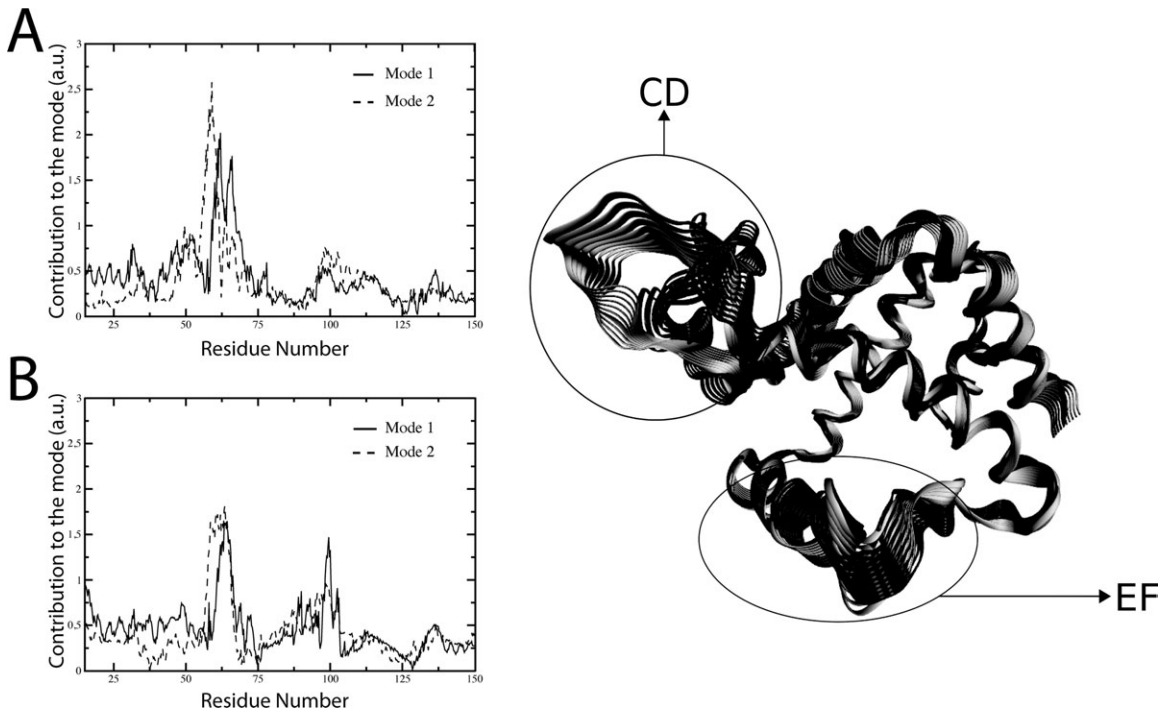

Figure 7

A and **B** represent the contribution of each residue to the first two transition essential modes (mode 1: solid line and mode 2: dashed line) for conformations A and B, respectively. Figure in the right is a representation of the transition essential modes. Results for conformations A and B are shown in black and gray, respectively. CD region and EF loop are showed in each case.

A6c–B5c with respect to both monomeric conformations. The overall result is that in the dimeric state given the structural asymmetry and negative cooperativity found in the time scale of the simulation the effective proportion of the 5c state increases with respect to the monomeric state.

DISCUSSION

Rice hemoglobin type 1 (rHb1) is a class 1 nonsymbiotic hemoglobin. Under physiological conditions, it behaves as a partially associated homodimer.[26] It has been shown that the residues that create the dimer interface in rHb1 are conserved among all the nsHbs. This suggests that the quaternary structure could play an important role in determining the chemical and biological behavior of this family of proteins.

In the present work quaternary structure proved to have a significant influence on the hexacoordination equilibrium. Our results for all possible combination of dimer states (5c-5c, 5c-6c, 6c-5c, and 6c-6c) simulation suggest that the flexibility of the CD region, the intersubunit interactions, and the conformation of key residue PheB10 are asymmetric and dependent on the other subunit coordination state. Free energy calculations for the dimer consistently revealed a strong dependence between the 5c to 6c equilibrium in one subunit and the other subunit coordination state. Specifically, while in subunit A the hexacoordination process seems to be poorly influenced by dimerization, the results for subunit B show that its 5c–6c equilibrium is strongly influenced by the coordination state of subunit A, in a negative

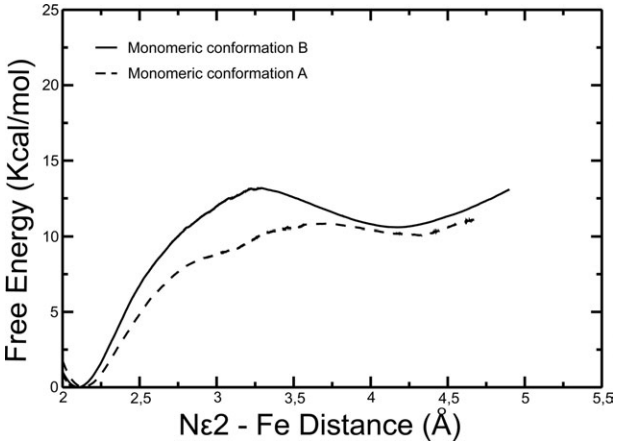

Figure 8

Free energy profile for the5c ↔ 6ctransition for the monomeric conformations A (A dashed line) and B (B solid line).

cooperativity scheme (i.e., 5c state is stabilized in subunit B, when subunit A is 6c or destabilized when subunit A is 5c).

The simulations of the monomeric structures maintain the asymmetry observed in the dimeric state in the time scale of our simulations. The differences between the dynamical properties of these two conformations are mainly related with the folding and flexibility of the CD region. In 5c-B and 6c-B, this region presents an unwound structure with very high flexibility, whereas in 5c-A and 6c-A, a stiffer structure with the characteristic C and D helices is observed. In addition, the results obtained from the ED analysis in the monomers suggest that the structural variation associated with the 6c↔5c process may involve a rearrangement in the CD region and in less extent the EF loop. Nevertheless, the free energy profiles for the 5c ↔ 6c transition in subunits A and B were similar.

Finally, the comparison between the free energy profiles for the hexacoordination process between the dimer and the monomers, indicates that dimerization tends to stabilize the 5c state in the mixed coordination states (i.e., A5c–B6c or A6c–B5c), thus reducing in this way the value of the hexacoordination equilibrium constant in the dimeric state. This suggests a key role played by the asymmetric properties of the dimeric protein in regulating the hexacoordination in the time scale of the simulation. These results could seem to present a discrepancy with the experimental work of Hargrove *et al.*[26] In the mentioned work, the authors have constructed a RiceHb1 mutant protein that is not able to form the dimeric state and measured the histidine binding and dissociation rate, obtaining very similar values than in the wild-type protein.[45] A possible reason for this discrepancy can rely on a protein concentration effect. However, it is also possible that the dynamical asymmetry would not be evidenced in ensemble-based solution experimental measurements.

In any case, the results obtained in this work suggest that the CD region may play an important role in regulating the 5c–6c equilibrium. Moreover, our results also show that the dimerization process in RiceHb1 affects this equilibrium, in part by modifying the CD region's structure and dynamics. These results add up to our previous observations which also highlighted the role played by the CD region in controlling the equilibrium in the archetypical globins, myoglobin and neuroglobin.[31,32] Thus, taken together, these results provide also evidence regarding the possible role of the CD region in the hexacoordination equilibrium in the classical 3-over-3 globins.

REFERENCES

1. Burmester T, Welch B, Reinhardt S, Hankeln T. A vertebrate globin expressed in the brain. Nature 2000;407:520–523.
2. Vinogradov SN, Hoogewijs D, Bailly X, Arredondo-Peter R, Gough J, Dewilde S, Moens L, Vanfleteren JR. A phylogenomic profile of globins. BMC Evol Biol 2006;6:31.
3. Vinogradov SN, Hoogewijs D, Bailly X, Arredondo-Peter R, Guertin M, Gough J, Dewilde S, Moens L, Vanfleteren JR. Three globin lineages belonging to two structural classes in genomes from the three kingdoms of life. Proc Natl Acad Sci USA 2005;102:11385–11389.
4. Jain R, Chan MK. Mechanisms of ligand discrimination by heme proteins. J Biol Inorg Chem 2003;8:1–11.
5. Olson JS, Phillips GN, Jr. Myoglobin discriminates between O_2, NO, and CO by electrostatic interactions with the bound ligand. J Biol Inorg Chem 1997;2:544–552.
6. Brunori M, Vallone B. Neuroglobin, seven years after. Cell Mol Life Sci 2007;64:1259–1268.
7. Burmester T, Ebner B, Weich B, Hankeln T. Cytoglobin: a novel globin type ubiquitously expressed in vertebrate tissues. Mol Biol Evol 2002;19:416–421.
8. Hargrove MS, Bruker EA, Stec B, Sarath G, Arredondo-Peter R, Klucas RV, Olson JS, Phillips GN, Jr. Crystal structure of a nonsymbiotic plant hemoglobin. Structure 2000;8:1005–1014.
9. Ioanitescu AI, Dewilde S, Kiger L, Marden MC, Moens L, Van Doorslaer S. Characterization of nonsymbiotic tomato hemoglobin. Biophys J 2005;89:2628–2639.
10. De Sanctis D, Pesce A, Nardini M, Bolognesi M, Bocedi A, Ascenzi P. Structure-functions relationships in the growing hexa-coordinate hemoglobin sub-family. IUBMB Life 2004;56:643–651.
11. Hoy JA, Hargrove MS. The structure and function of plant hemoglobins. Plant Physiol 2008;46:371–379.
12. Taylor ER, Nie XZ, Alexander WM, Hill RD. A cereal haemoglobin gene is expressed in seed and root tissue under anaerobic conditions. Plant Mol Biol 1994;24:853–862.
13. Trevaskis B, Watts RA, Andersson CR, Llewellyn DJ, Hargrove MS, Olson JS, Dennis ES, Peacock WJ. Two hemoglobin genes in *Arabidopsis thaliana*: the evolutionary origins of leghemoglobins. Proc Natl Acad Sci USA 1997;94:12230–12234.
14. Smagghe BJ, Sarath G, Ross E, Hilbert JL, Hargrove MS. Slow ligand binding kinetics dominate ferrous hexacoordinate hemoglobin reactivities and reveal differences between plants and other species. Biochemistry 2006;45:561–570.
15. Smagghe BJ, Hoy JA, Percifield R, Kundu S, Hargrove MS, Sarath G, Hilbert JL, Watts RA, Dennis ES, Peacock WJ, Dewilde S, Moens L, Blouin GC, Olson JS, Appleby CA. Review: correlations between oxygen affinity and sequence classifications of plant hemoglobins. Biopolymers 2009;91:1083–1096.
16. Arredondo-Peter R, Hargrove MS, Sarath G, Moran JF, Lohrman J, Olson JS, Klucas RV. Rice hemoglobins. Gene cloning, analysis, and O2-binding kinetics of a recombinant protein synthesized in *Escherichia coli*. Plant Physiol 1997;115:1259–1266.
17. Duff SM, Wittenberg JB, Hill RD. Expression, purification, and properties of recombinant barley hemoglobin (*Hordeum sp.*) hemoglobin. Optical spectra and reactions with gaseous ligands. J Biol Chem 1997;272:16746–16752.
18. Hoy JA, Robinson H, Trent JT, III, Kakar S, Smagghe BJ, Hargrove MS. Plant hemoglobins: a molecular fossil record for the evolution of oxygen transport. J Mol Biol 2007;371:168–179.
19. Hill RD. What are hemoglobins doing in plants? Can J Bot 1998;76:707–712.
20. Kundu S, Premer SA, Hoy JA, Trent, III, Hargrove MS. Direct measurement of equilibrium constants for high-affinity hemoglobins. Biophys J 2003;84:3931–3940.
21. Vinogradov SN, Hoogewijs D, Bailly X, Arredondo-Peter R, Gough J, Dewilde S, Moens L, Vanfleteren JR. A phylogenetic profile of globins. BMC Evol Biol 2006;6:31.
22. Lira-Ruan V, Sarath G, Klucas RV, Arredondo-Peter R. Synthesis of hemoglobins in rice (*Oryza sativa* var. Jackson) plants growing in normal and stress conditions. Plant Sci 2001;161:279–287.
23. Ross EJ, Stone JM, Elowsky CG, Arredondo-Peter R, Klucas RV, Sarath G. Activation of the Oryza sativa non-symbiotic haemoglobin-2 promoter by the cytokine-regulated transcription factor, ARR1. J Exp Bot 2004;55:1721–1731.

24. Ohwaki Y, Kawagishi-Kobayashi M, Wakasa K, Fujihara S, Yoneyama T. Induction of class-1 non-symbiotic hemoglobin genes by nitrate, nitrite and nitric oxide in cultured rice cells. Plant Cell Physiol 2005;46:324–331.
25. Weiland TR, Kundu S, Trent JT, III, Hoy JA, Hargrove MS. Bishistidyl hexacoordination in hemoglobins facilitates heme reduction kinetics. J Am Chem Soc 2004;126:11930–11935.
26. Goodman MD, Hargrove MS. Quaternary structure of rice nonsymbiotic hemoglobin 2001;276:6834–6839.
27. Smagghe BJ, Kundu S, Hoy JA, Halder P, Weiland TR, Savage A, Venugopal A, Goodman M, Premer S, Hargrove MS. Role of phenylalanine B10 in plant nonsymbiotic hemoglobins. Biochemistry 2006;45:9735–9745.
28. Goodsell DS, Arthur JO. Structural symmetry and protein function. Annu Rev Biophys Biomol Struct 2000;29:105–53.
29. Swapna LS, Srikeerthana K, Sirinivasan N. Extent of structural asymmetry in homodimeric proteins: prevalence and relevance. PLoS ONE 2012;7:e36688.
30. Hughes SJ, Tanner JA, Hindley AD, Miller AD, Gould IR. Functional asymmetry in the lysl-tRNA synthetase explored by molecular dynamics, free energy calculations and experiment. BMC Structural Biology 2003;3:5.
31. Capece L, Marti MA, Bidon-Chanal A, Nadra A, Luque FJ, Estrin DA. High pressure reveals structural determinants for globin hexacoordination: neuroglobin and myoglobin cases. Proteins 2009;75: 885–894.
32. Nadra DA, Marti MA, Pesce A, Bolognesi M, Estrin DA. Exploring the molecular basis of heme coordination in human neuroglobin. Proteins 2008;695–705.
33. Berendsen HJC, Postma JPM, Van Gunsteren WF, DiNola A, Haak JR. Molecular dynamics with coupling to an external bath. J Chem Phys 1984;81:3684–3690.
34. Cheatham lii TE, Cieplak P, Kollman PA.A modified version of the Cornell et al. force field with improved sugar pucker phases and helical repeat. J Biomol Struct Dyn 1999;16:845–862.
35. Marti MA, Crespo A, Capece L, Boechi L, Bikiel DE, Scherlis DA, Estrin DA. Dioxygen affinity in heme proteins investigated by computer simulation. J Inorg Biochem 2006;100:761–770.
36. Bidon-Chanal A, Marti MA, Crespo A, Milani M, Orozco M, Bolognesi M, Luque FJ, Estrin DA. Ligand-induced dynamical regulation of NO conversion in *Mycobacterium tuberculosis* truncated hemoglobin-N. Proteins 2006;64:457–464.
37. Pearlman DA, Case DA, Caldwell JW, Ross WS, Cheatham TE, III, DeBolt S, Ferguson D, Seibel G, Kollman P. AMBER, a package of computer programs for applying molecular mechanics, normal mode analysis, molecular dynamics and free energy calculations to simulate the structural and energetic properties of molecules. Comput Phys Commun 1995;91:1–41.
38. Amadei A, Linssen ABM, Berendsen HJC. Essential dynamics of proteins. Proteins Struct Funct Genet 1993;17:412–425.
39. Marti MA, Estrin DA, Roitberg AE. A molecular basis for the pH dependent structural transition of nitrophorin 4. J Phys Chem B 2009;113:2135–2142.
40. Jarzinski C. Nonequilibrium equality for free energy differences. Phys Rev Lett 1997;78:2690–2693.
41. Meuwly M, Becker OM, Store R, Karplus M. NO rebinding to myoglobin: a reactive molecular dynamics study. Biophys Chem 2002;98:183–207.
42. Marti MA, Bidon-Chanal A, Crespo A, Yeh S, Guallar V, Luque FJ, Estrin DA. Mechanism of Product Release in NO detoxification from Mycobacterium tuberculosis Truncated Hemoglobin N. J Am Chem Soc 2008;130:1688–1693.
43. Capece L, Estrin DA, Marti MA. Dynamical characterization of the heme NO oxygen binding (H-NOX) domain. Insight into soluble guanylate cyclase allosteric transition. Biochemistry 2008;47:9416–9427.
44. Rodriguez R, Ferreiro DN, Toitberg AE, Marti MA, Turjanski AG. P38g Activation triggers dynamical changes in allosteric docking sites. Biochemistry 2011;50:1384–1395.
45. Hargrove M. A flash photolysis method to characterize hexacoordinate hemoglobin kinetics. Biophys J 2000;79:2733–1042.